Marine sediment transport

de Vries, Sierd; Wengrove, Meagan; Bosboom, Judith

DOI
10.1016/B978-0-08-102927-5.00009-6

Publication date
2020

Document Version
Final published version

Published in
Sandy Beach Morphodynamics

Marine sediment transport

9

Sierd de Vries[a], *Meagan Wengrove*[b], *Judith Bosboom*[a]
[a]Department of Hydraulic Engineering, Delft University of Technology, Delft, The Netherlands; [b]Oregon State University, Corvallis, OR, United States

Chapter outline

9.1 Introduction

Sediment transport on sandy beaches connects hydrodynamic conditions to changes in morphology. Sediment transport is typically driven by a combination of hydrodynamic mechanisms, which include waves, wind and tides. The mechanisms vary in both magnitude and direction on different spatiotemporal scales. For instance, flows due to wind, tides and the net effect of waves can typically vary over a timescale of several hours and more, whereas the orbital motion of waves varies over a timescale of seconds, and turbulent fluctuations over milliseconds.

Independent of the scale of interest, the volume of sediment transported in a water column (or through the air) per unit width can be defined as a horizontal vector (S [m^2 s^{-1}]) resulting from the product of a sediment concentration (expressed as a ratio of sediment volume to total volume c_s [m^3 m^{-3}]) and horizontal sediment speed (u_s [m s^{-1}]) integrated over the vertical water (air) column:

$$S = \int_0^h c_s u_s dz \tag{9.1}$$

where the vertical coordinate z varies from the bed at $z = 0$ to the water surface where $z = h$.

Sandy Beach Morphodynamics. http://dx.doi.org/10.1016/B978-0-08-102927-5.00009-6

Many uncertainties exist in the detailed relationship between the hydrodynamic conditions, the sediment concentration, the sediment speed and therefore the sediment transport at different scales. It is far from straightforward to perform comprehensive and repeatable measurements of spatiotemporally varying sediment speeds and sediment concentrations. Due to both the complexity of transport mechanisms and the limited availability of such direct measurements of transport, the total understanding of sediment transport and driving processes of sediment transport is still under development. There are, however, many useful theoretical and practical concepts available that describe and quantify sediment transport at different scales of interest.

The magnitude of sediment transport can vary in many ways due to feedbacks with environmental processes and morphology. An accepted model concept is that the carrying capacity of water flow over a flatbed is related to the (local) flow velocity to some power higher than 1. Also, time-varying horizontal gradients in sediment transport cause morphological changes following continuity according to:

$$\frac{\partial \eta}{\partial t} = -\frac{1}{(1-a)}\left(\frac{\partial S_x}{\partial x} + \frac{\partial S_y}{\partial y}\right) \tag{9.2}$$

where η is the surface elevation of the bed, S_x and S_y are the time- and space-dependent sediment transports in x- and y-direction respectively and a is the porosity (Parker et al., 2000). When transport gradients in the direction of the transport are positive, the increasing transport leads to erosion at the bed. When transport gradients in the direction of the transport are negative, the decreasing transport leads to sedimentation at the bed.

A steady concentration (and associated sediment transport) seems to exist in stationary and uniform conditions, which simplifies the description of sediment transport. However, at sandy beaches the conditions are hardly stationary or uniform with both sediment concentrations and sediment speed responding differently to changing flow due to waves and currents combined and changing morphology. Therefore, more complex concepts are needed to describe sediment transport and gradients on beaches.

This chapter describes the most common concepts of sediment transport at sandy beaches. It starts with some essential details on timescales and sediment properties that are important for sediment transport, followed by the dominant modes of sediment transport, bedload and suspended load. Furthermore, alongshore sediment transport and cross-shore sediment transport are discussed separately. This chapter closes with a reflection on some of the current challenges regarding the description of sediment transport processes.

9.1.1 Timescales of sediment transport

The range of timescales that characterise sediment transport at sandy beaches can be classified according to the hydrodynamic forcing. The most important forcings and timescales are:

- turbulence (milliseconds)
- intra-wave processes on the short wave and wave group scale (seconds)
- short-wave-averaged flow (minutes–hours).

Turbulence is a relatively small-scale instability generated by shear. Turbulence in the water column affects the pathways of individual sediment grains on a very small scale (μm–cm). Describing the details of turbulence in flows remains a scientific challenge. Therefore, when measuring and modelling sediment transport, the turbulent timescale is often addressed using parameterisations of turbulent shear through an eddy viscosity concept of water that is linked to sediment dispersion.

Sediment transport on the intra-wave timescale (centimetres–metres) is driven by oscillatory flows that are related to the orbital motion of the waves. Such orbital flows include opposite directions depending on phases within the wave cycle. The resulting sediment transport can have a net component over the wave cycle that adds to a wave-averaged transport.

Sediment transport on a wave-averaged timescale (1–10 m) is also driven by wave-averaged flows due to wind, wave-induced radiation stress gradients, tides, wave streaming and Stokes drift. The magnitude and direction of wave-averaged flows can vary significantly in magnitude up to several metres per second and direction (with alongshore and cross-shore components) such as explained in Chapter 7 and summarised in Fig. 9.1.

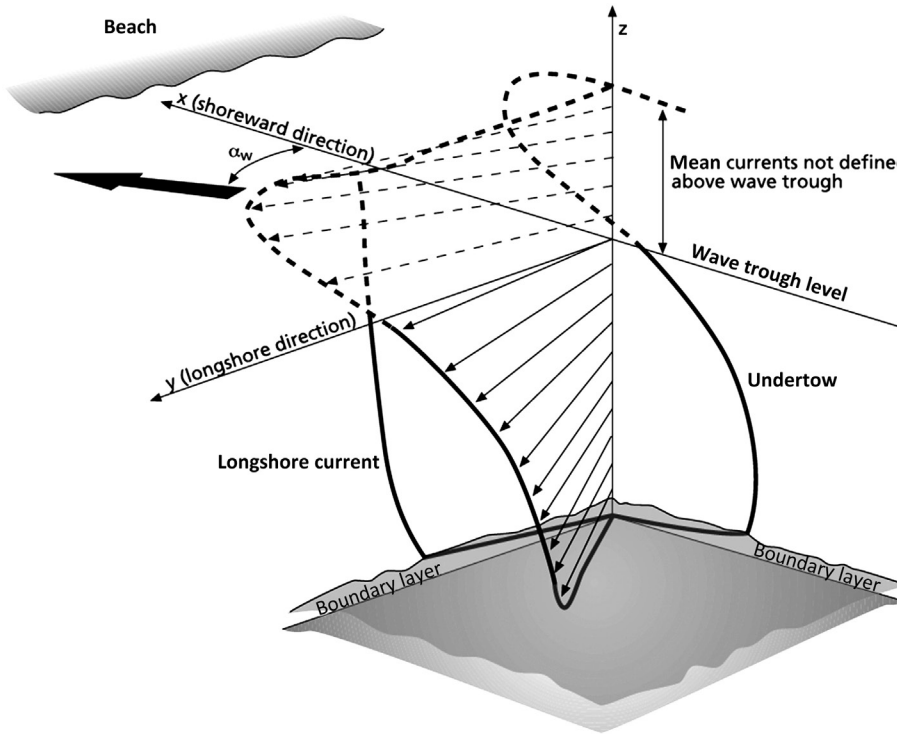

Figure 9.1 Schematic overview of wave-averaged currents in alongshore and cross-shore direction.
Source: Data from Svendsen and Lorenz, 1989.

There is ongoing interaction between the different sediment transport timescales. For instance, oscillatory near-bed turbulent flows are not only responsible for stirring up sediment at the intra-wave scale but they also influence the wave-averaged sediment concentrations that are important for transport driven by wave-averaged flows.

9.2 Sediment properties

Important parameters for the sediment transport process are the mobility of sediment particles expressed by the initiation of motion together with the sediment particle's fall velocity. Both parameters are dependent on grain size, weight and shape. In the case of sandy beaches, a mix of grain sizes and shapes is usually present, forming a grain size distribution (see Chapter 2 for more elaborate discussion on sediment properties). In sediment transport concepts, a median grain size diameter is often chosen as a representative value for the distribution (D). For simplicity, a single grain size, unless otherwise stated, is used throughout this chapter.

9.2.1 Initiation of motion

The initiation of motion of a single grain can be schematised by a balance of forces on sediment particles. The fluid motion causes a drag force and a lift force on individual grains. The mobilising force is counteracted by the gravitational force on the grain (see Fig. 9.2).

The Shields (Shields, 1936) parameter (θ) summarises the ratio between mobilizing and stabilizing forces on a single sediment grain according to:

$$\theta = \frac{\tau_b}{(\rho_s - \rho)\, gD} \tag{9.3}$$

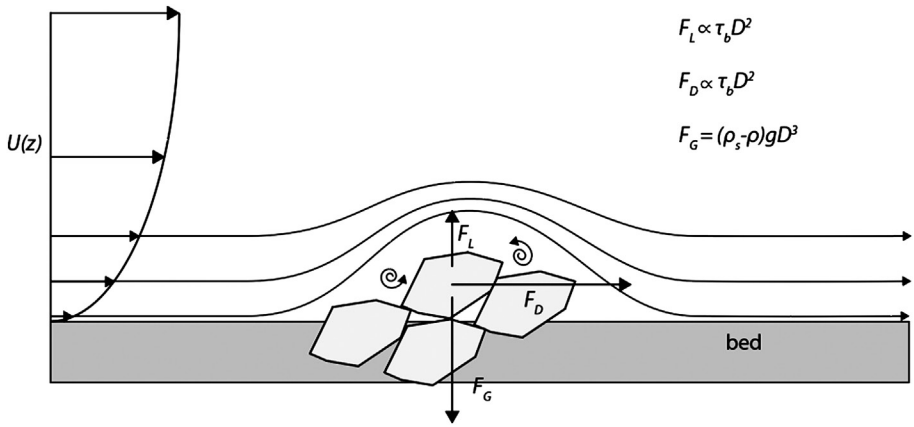

Figure 9.2 Forces on grains on the bed. Assuming spherical sediment grains, the proportionality of the forces can be estimated by the equations indicated in the figure.

where τ_b is the shear stress exerted by the fluid flow on the grain, $(\rho_s - \rho)$ is the density difference between the sediment grain (ρ_s) and water (ρ), g is the gravitational acceleration and D is the grain size diameter.

A critical Shields parameter (θ_{cr}) and associated critical shear stress ($\tau_{b,cr}$) determine the threshold of motion for a specific sediment weight and diameter. In a series of famous experiments, Shields (1936) has determined the critical Shields parameter to be around $\theta_{cr} = 0.05$ for sand that was placed on a horizontal bed in the case of a uniform flow. Also, Shields found the critical Shields parameter to be weakly dependent on the grain Reynolds number.

In addition to the Reynolds dependency, typical circumstances related to sandy beaches can influence the threshold of motion. Those circumstances involve bed slopes, oscillatory flows, bed ripples and the grading of sediment. Bed slopes in the direction of the current can cause the critical Shields parameter to be higher for upward slopes and lower for downward slopes. Oscillatory flows involve peak velocities that can exceed the threshold of motion. The wave-induced near-bed peak velocities are sometimes added to the current velocities to determine an equivalent wave-related Shields parameter (θ_{eq}). The time-dependent process related to grain size selective sediment transport, the sheltering of small grains by larger grains and grain angularity can influence the threshold of motion in the case of graded sediments.

9.2.2 Sediment fall velocity

The sediment fall velocity in water (w_f) is a constant velocity that is characterised by a downward gravitational acceleration that is in balance with the upward drag force. In the case of spherical sediment particles this equates to:

$$w_f = \sqrt{\frac{4(s-1)gD}{3C_f}} \tag{9.4}$$

where s is the relative density of sediment defined by $s = \rho_s / \rho$; C_f is the drag coefficient of the sediment particle which is found to be dependent on the grain Reynolds number. Sediment fall velocities roughly vary between 0.005 and 0.06m s^{-1} when a typical range of sediment is considered from 50 to 400 µm. Detailed relationships between the grain size and fall velocities have been formulated amongst others by van Rijn (1993). An example is given in Fig. 9.3.

9.3 Modes of sediment transport

Typical modes of sediment transport are bedload and suspended load. Bedload sediment transport occurs typically very close to the bed where forces between sediment grains dominate the transport mechanism. Suspended load is the transport of sand above the bedload layer up to the water surface generally assumed to be carried by the upward turbulent diffusive forces. A common modelling approach is based on the

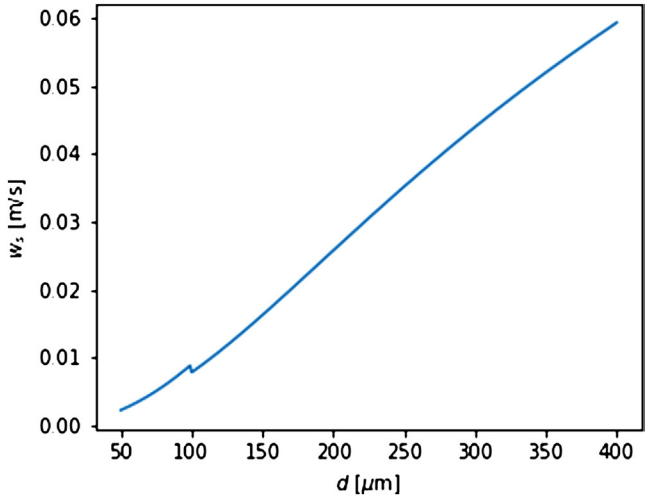

Figure 9.3 The dependency between fall velocity and grain size formulated by Van Rijn (1993).

discrimination between the instantaneous response of sediment transport (sediment concentration and sediment speed) to changes in near-bed intra-wave flow velocities in the case of bedload and the wave-averaged changes in sediment concentration over the entire water column in the case of suspended load. The sum of both bedload and suspended load represents the total load of sediment in the water column due to hydrodynamic forcing. See Fig. 9.4 for a conceptual representation in the case of uniform flow and the more complex case of cross-shore wave-averaged flow conditions.

9.3.1 Suspended load and the advection diffusion approach

Sediment suspensions typically occur in turbulent zones where waves break. Horizontal flow velocities advect the sediment that is in suspension assuming that sediment speed is equal to the flow velocity. Sediments are brought into suspension from the bed by upward turbulent velocities against the downward fall velocity of the sediments.

Suspended load can be described by a 3D advection diffusion framework assuming the conservation of sediment:

$$\frac{\partial c}{\partial t}+u\frac{\partial c}{\partial x}+v\frac{\partial c}{\partial y}+(w-w_f)\frac{\partial c}{\partial z}-\frac{\partial\left(\varepsilon_h\frac{\partial c}{\partial x}\right)}{\partial x}-\frac{\partial\left(\varepsilon_h\frac{\partial c}{\partial y}\right)}{\partial y}-\frac{\partial\left(\varepsilon_v\frac{\partial c}{\partial z}\right)}{\partial z}=0 \tag{9.5}$$

where the horizontal sediment velocities (u_s, v_s) are assumed equal to the water velocity (u, v) and the vertical sediment velocity (w_s) is assumed the difference between water velocity (w) and sediment fall velocity (w_f). Coefficients ε_h and ε_v represent the horizontal and vertical dispersion (or diffusivity) of sediment, respectively. Note that

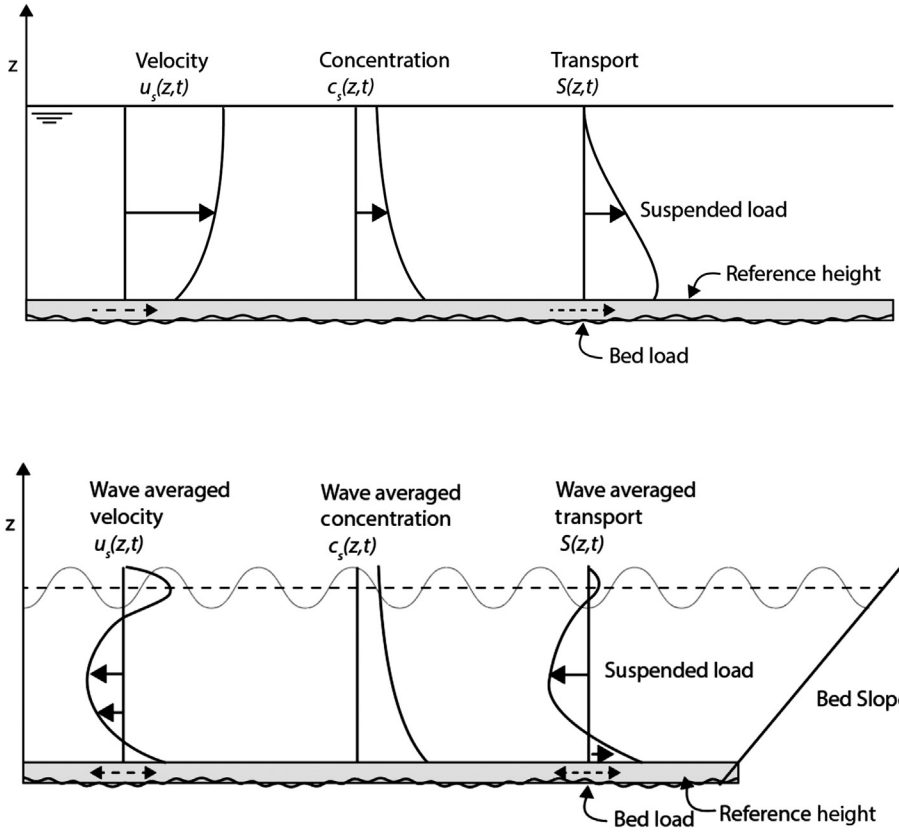

Figure 9.4 Top panel shows a conceptual representation of sediment transport as a function of sediment velocity and sediment concentration assuming homogeneous flow. The bottom panel shows a conceptual representation of a typical wave-averaged cross-shore sediment transport under combined (non-breaking) wave and current forcing in a confined cross-shore profile. Note the cross-shore flow variations over depth.

the dispersion coefficients can, depending on the considered scale and detail of measurements or model, reflect several processes implicitly that typically involve smaller scales than the ones that are explicitly reflected by the advection terms. For instance, when interpreting measurements of sediment transport one can measure the advection of local sediment vortices on a very detailed scale over a rippled bed (using high-frequency PIV systems) leading to large advection terms in the high-resolution advection diffusion description. Alternatively, one can measure average flow velocities and concentration gradients in a larger control volume (using an array of acoustic devices) leading to larger dispersion coefficients in the equation and smaller advection terms representing less detail.

A time-invariant wave-averaged vertical sediment concentration profile can occur when flows and sediment properties are not varying (or very slowly varying) in time

and no horizontal gradients in sediment concentration exist. With the time-averaged upward sediment dispersion in balance with the downward fall velocity, Eq. (9.5) can be rewritten as:

$$w_f c - \varepsilon_v \frac{\partial c}{\partial z} = 0 \tag{9.6}$$

which allows for the estimation of a steady vertical concentration profile:

$$c(z) = c_a \exp\left(-\int_a^h \frac{w_f}{\varepsilon_v} \partial z \right) \tag{9.7}$$

where c_a is a reference concentration at height a which is commonly assumed to be the horizontal interface between the bedload and suspended load (see Fig. 9.4). The sediment dispersion is a fundamental parameter for the estimation of the concentration profile, and it is a function of bottom roughness and shear stress, sediment stirring due to waves and settling velocity. A relation between eddy viscosity is often adopted when determining the dispersion coefficient. However, the dispersion of sediment is arguably not entirely analogous to the eddy viscosity of water (Camenen and Larson, 2007). Different estimations of the sediment dispersion profile have been derived using data which can be used for modelling. Common examples are the constant, linear and parabolic dispersion profiles (see Fig. 9.5).

Where the constant dispersion profile is easiest for modelling purposes from a pragmatic point of view, the theoretical shape of an eddy viscosity profile of water flow in an open channel is followed by the parabolic dispersion profile. The increased dispersion of sediment due to increased turbulence at the water level due to wave breaking can be reflected by the linear distribution. In addition to Fig. 9.5, more complex empirical estimations of dispersion profiles have been formulated when simulating sediment transport with both waves and current profiles. A widely used example in numerical models is the empirical formulation by van Rijn (1993) who makes a discrete separation between current-related dispersion and wave-related dispersion and used empirical estimates for the shape of the distribution, including a maximum and minimum dispersion.

The reference concentration at height a is dependent on shear stress, sediment parameters and bed roughness. From a practical point of view, the assumed reference concentration has a crucial effect on the estimation of the total sediment load in the water column regardless of the shape of the chosen dispersion profile. A comprehensive overview of the different formulations is given in Camenen and Larson (2007).

Naturally, the reference concentration and reference level are related to the bedload transport and bedload layer thickness. Often the reference level and the top of the bedload layer are considered equal. Furthermore, reference concentrations are formulated as higher order functions of the near-bed shear stress or shear velocity similar to common bedload transport formulations.

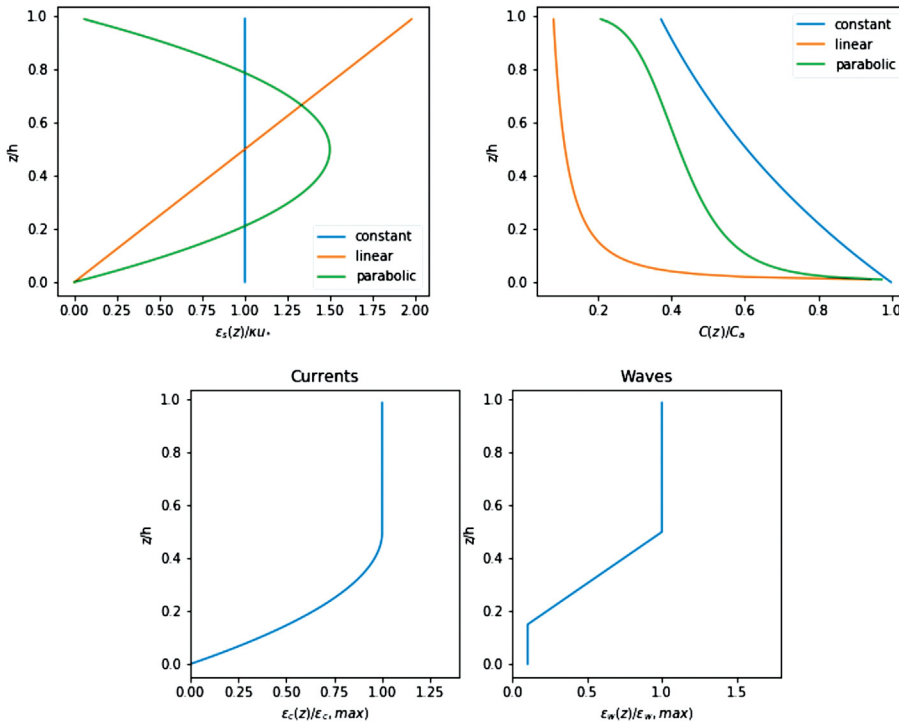

Figure 9.5 Top left: the depth-varying dispersion profiles assuming constant, linear and parabolic profiles normalised with a common reference that is dependent on shear stress. Top right: the resulting concentration profiles. Bottom panels show the current-related dispersion and wave-related dispersion proposed by Van Rijn (1993) and widely implemented in numerical models such as Delft3D.

9.3.2 Bedload transport

Bedload transport involves moving sediment in the thin layer where transported sediments are in close contact with the bed, and sediment concentrations respond immediately to changes in flow velocities (Nielsen, 1992). Considering the specific case of sandy beaches, bedload is the dominant mechanism outside the surf zone where the turbulent forces that are required for suspended load are limited, and near-bed shear orbital velocities due to waves are generally relatively large compared to wave-averaged currents. Bedload transport is a large contributor to the total load throughout the surf zone in both stormy and mild conditions. The momentum exchange is driven by the near-bed velocity structure, which is a function of both the bed shear stress, or the friction force between the fluid and the bed (τ_b), and pressure gradient induced by passing waves ($\mathrm{d}p/\mathrm{d}x$) (Shields, 1936; Sleath, 1999).

Shear controls the momentum transfer through the wave and current boundary layers to the bed, where a lateral force imposed on the sediment grains causes the grains to move. Shear-driven transport can be characterised by the non-dimensional

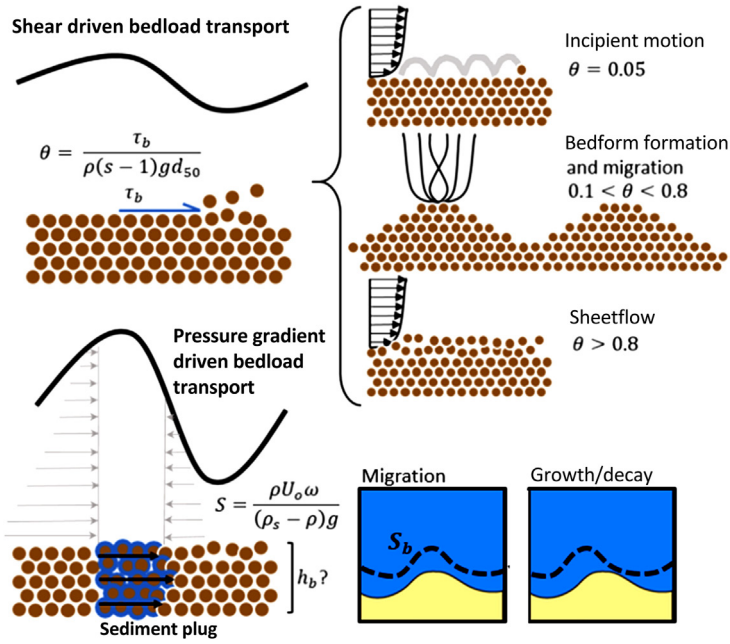

Figure 9.6 Mechanisms of bedload sediment transport. Shear (top) versus pressure gradient-induced (bottom left) sediment transport. Note, shear-driven transport mechanics (incipient motion, bedform formation/migration and sheet flow) are relevant to both wave- and current-driven flows, whereas pressure gradient-driven transport is most relevant to wave-driven flow. Mechanism for bedform migration and growth (bottom right). When the transport is in phase with the bedform shape, the bedform will migrate; when out of phase, the bedform will grow (phase offset to the left of bedform crest—shown) or decay (phase offset to the right of bedform crest—not shown).

bed stress or the Shields parameter (θ; Eq. (9.3)). Bedload occurs when θ exceeds the threshold of incipient motion or the critical Shields parameter θ_{cr} ($\theta > 0.05$), such that grains start to roll and bounce along the bed. Sand ripples and bedforms form, move and grow when $\sim 0.1 < \theta < \sim 0.8$. Sheet flow occurs when $\theta > 0.8$ and is characterised with high and mobile sediment concentrations close to the bed (Fig. 9.6). Many sediment transport models rely on an estimate of the bed shear stress either determined through measurements (which are difficult in the field) or estimate the bed shear stress with a friction factor model. Friction factor models estimate the bed stress under waves, currents or combined flows by multiplying the squared flow velocity by a friction factor fit from empirical data or detailed intra-wave models.

Pressure gradient-induced transport is characterised by a ratio between the destabilizing forces applied by the peak horizontal pressure gradient and the stabilizing forces applied by gravity, such that the non-dimensional Sleath parameter is:

$$S_l = \frac{\rho U_0 \omega}{(\rho_s - \rho)g} \tag{9.8}$$

where the horizontal pressure gradient for sinusoidal waves can be described by $dp(t)/dx = \rho U_o \omega \sin(\omega t)$, ω is the angular frequency, U_o is the wave orbital velocity amplitude, ρ_s is the grain density, ρ is the water density and the ratio is not dependent upon sediment grain size (Foster et al., 2006; Sleath, 1999). During pressure gradient-induced transport the sediment structure will momentarily fluidize, and the sediment will move as a plug (Fig. 9.6). Pressure gradient-induced sediment transport, or plug flow, occurs when the Sleath parameter exceeds a critical value of approximately 0.29. Knowledge of the influence of the pressure gradient is limited by understanding of the mobile layer thickness, h_b (Fig. 9.6). At the grain scale, sediment transport is driven by a complex combination of both shear and pressure gradient-induced forces (Foster et al., 2006; Frank et al., 2015; Mieras et al., 2017; Yeh and Mason, 2014).

Estimating the magnitude of bedload sediment flux is difficult using metrics of the Shields parameter and the Sleath parameter. Furthermore, analytical solutions for the bedload sediment transport flux are not well defined due to challenges in modelling sediment speed, the distribution of the sediment concentration and the mobile layer thickness (h_b) in relation to the flow forcing conditions. Instead, there are many empirical and semi-empirical approaches based on estimations of the total bedload transport in wave, current and combined wave-current forcing conditions using measurements. Generally, bedload sediment transport models depend on both the flow forcing condition and the granular or bedform roughness.

Models that are formulated to quantify bedload sediment transport can be a function of the bed shear stress or directly a function of the flow velocity. The bed shear stress is indirectly related to the flow velocity through the boundary friction velocity (u_*) which is dependent on the vertical velocity profile. The bed shear stress τ_b is related to the square of the flow velocity:

$$\tau_b = \rho u_*^2 \sim u^2 \tag{9.9}$$

Empirical findings from experiments in both predominantly wave and riverine current-driven flows show that bedload sediment transport, S_b, is related to some higher order function ($n > 1$) of bed shear stress by:

$$S_b \sim \tau_b^n \tag{9.10}$$

Therefore, it is generally accepted that S_b has a higher order (i.e. non-linear) relationship with the horizontal flow velocity.

While Eq. (9.10) is initially derived for riverine currents, they are also successfully applied to the oscillatory motion of waves. The assumption that the instantaneous sediment transport is proportional to some power of the instantaneous near-bed orbital velocity for waves or the mean velocity for currents is called the quasi-steady approach (see, for instance, Grasmeijer, 2002). In oscillatory flows, the net bedload transport rate over a wave period can be obtained by time averaging (over the wave period, T) of the instantaneous transport rate using a bedload transport formula 'quasi-steady approach'.

The conceptualisation of bedload transport can be specified using shear based models and energetics models and adopting the terminology by Ribberink (1998) and Wengrove et al. (2019). Shear-based models involve a detailed description of the mobilizing fluid shear and stabilizing properties of the sediment grain. Energetics models consider the energy dissipation by shear as the main driver for sediment transport.

9.3.2.1 *Shear approach to total bedload*

Shear-based bedload models typically relate the bedload sediment flux (S_b in volume of solid material per time unit) to the excess non-dimensional bed stress. In its traditional form, valid for unidirectional flow, it is written as:

$$S_b = m\left(\theta - \theta_c\right)^n D\sqrt{gD^3\left(s-1\right)} \tag{9.11}$$

where Meyer-Peter and Muller (1948) determined $m = 8$ and $n = 1.5$ as an example of a shear-based bedload sediment transport model derived for riverine environments.

Eq. (9.11) has been adapted for wave applications as well, either by using a wave-averaged shear stress or by accounting for the intra-wave variation of the shear stress (Ribberink, 1998). In order to cope with oscillatory flows, Ribberink (1998) described bedload transport by writing Eq. (9.11) in a time-dependent (intra-wave) form, which enables a sign change during the wave cycle:

$$S_b\left(t\right) = m\left\langle\left(\left|\theta\left(t\right)\right| - \theta_c\right)^n \frac{\theta\left(t\right)}{\left|\theta\left(t\right)\right|} D\sqrt{gD^3\left(s-1\right)}\right\rangle \tag{9.12}$$

where θ is the time-dependent instantaneous Shield parameter during the wave cycle, |...| is the absolute magnitude and <...> is the averaging over the wave scale.

This resulting quasi-steady model determines the wave-averaged, wave-related transport while assuming an instantaneous response of the sediment to the time-varying bed shear-stress. Herewith it takes wave nonlinearities into account to the extent that wave skewness leads to a net transport in wave-propagation direction. In addition to wave skewness, acceleration differences between the front and the back of the wave exist that can influence the wave-related bedload transport (van der A et al., 2013). Since waves in the nearshore are generally asymmetric or skewed, and velocity asymmetry and skewness have been correlated to bedload sediment transport magnitudes, the consideration of the wave shape in the context of bedload sediment transport is important.

These shear-based bedload sediment transport models are dependent upon an external estimate of the bed shear stress, mainly estimated through friction factor-based models. Some bed shear stress models assume a logarithmic boundary layer shape, which is not necessarily representative for many nearshore flows, where waves and combined wave-currents complicate the boundary layer structure and momentum exchange. In addition, there are several bedload sediment transport models that are still considered to be shear-based but, instead of using an external shear formulation, each

is embedded with its own shear stress model. van Rijn (2007, 1993) commonly used wave-averaged models of this functional form.

The application of the shear theories has led to a wide range of models that are each very sensitive to the detailed assumptions regarding sediment transport and the assumptions regarding the shear stresses (and threshold shear stresses). For instance, in Eqs. (9.11) and (9.12) it is required to calibrate not only for n, m but also for the shear model that is behind θ (including currents and intra-wave processes). At the same time, such models are often calibrated on total sediment transport alone. In specific cases, results of different shear-based models are shown to expose large variabilities when compared to measurements (Wengrove et al., 2019). By implication, considerable uncertainty should be expected if untuned models are used to make absolute predictions for field conditions.

9.3.2.2 Energetics approach to bedload (Bagnold, Bailard, Bowen line of models)

Energetics models relate the sediment transport to some portion of energy dissipation by the flow (Bagnold, 1966; Bailard, 1981; Bailard and Inman, 1981; Bowen, 1980). For bedload, the energy dissipation is due to bed friction, which is modelled through a quadratic friction law. Consequently, in energetics models, the bedload transport is related to a higher order function of the flow velocity. As for the shear-based models, appropriate friction factors need to be specified. As opposed to the shear-based models, there is no criterion for the initiation of motion through a critical bed shear stress. Bagnold (1966) formulated an energetics bedload (and suspended load) model for unidirectional flow on a sloping bed. The model style for total load transport was extended to a quasi-steady formulation by Bowen (1980) and Bailard and Inman (1981) valid for combined wave current flow on a sloping bed. A recent example by Hsu et al. (2006) involves a horizontal bed and slight reformulation of the transported volume of solid material (S_b) due to waves and currents:

$$S_b = C_w \frac{\epsilon_b}{\tan\varphi\,(s-1)\,g}\left\langle \left|\tilde{\vec{U}}_0\right|^2 \tilde{U}_0 \right\rangle + C_c \frac{\epsilon_b}{\tan\varphi\,(s-1)\,g}\left\langle \left|\vec{U}_0\right|^2 \bar{U}_0 \right\rangle \tag{9.13}$$

where $\left|\tilde{\vec{U}}_0\right|$ is the magnitude of the orbital velocity, $\tilde{U}_0$ is the orbital velocity, $\left|\vec{U}_0\right|$ is the magnitude of the orbital and current velocity, $\bar{U}_0$ is the current velocity and φ is the angle of repose. Additionally, ϵ_b is the sediment transport efficiency, which can be seen as the efficiency of the process of momentum transfer from the fluid to moving the sand. Finally, C_w and C_c are the wave and combined-wave current friction coefficients, respectively. Those friction coefficients depend on the existence of bedforms such as sandbars and bed ripples (see for details Hsu et al., 2006; Wengrove et al., 2019).

In fieldwork and modelling efforts where the boundary layer dynamics are not well resolved, without high-resolution measurements or modelling of boundary layer shape, it has been shown that the energetics method of estimating sediment transport can provide robust results (Hoefel and Elgar, 2003; Hsu et al., 2006; Wengrove

et al., 2019). However, the bed shear stress along with the pressure gradient are ultimately the mechanisms moving the sediment grains, so with high fidelity estimates of the bed shear stress, shear-based models are also shown to perform (Rodríguez-Abudo and Foster, 2014). Clearly, bedload sediment transport models are still largely empirical and the value of quantitative estimates depends widely on measurements that are only rarely available in the field.

9.4 Alongshore and cross-shore sediment transport

In the nearshore both currents and waves influence the magnitude and direction of sediment transport in the alongshore and the cross-shore directions. Often the two motions are separated in process descriptions. It is important to note that all discussed processes are ultimately a function of the combination of wave and current forcing, although for the purpose of simplification some processes are described as systematically driven by currents or waves individually. Fig. 9.7 shows the dominant sediment transport processes along the cross-shore profile for both suspended and bedload sediment transport as well as the corresponding distribution of alongshore sediment transport.

9.4.1 Alongshore sediment transport

Alongshore sediment transport is mainly driven by obliquely incident waves that stir up the sediment and generate an alongshore current transporting the sediment. The

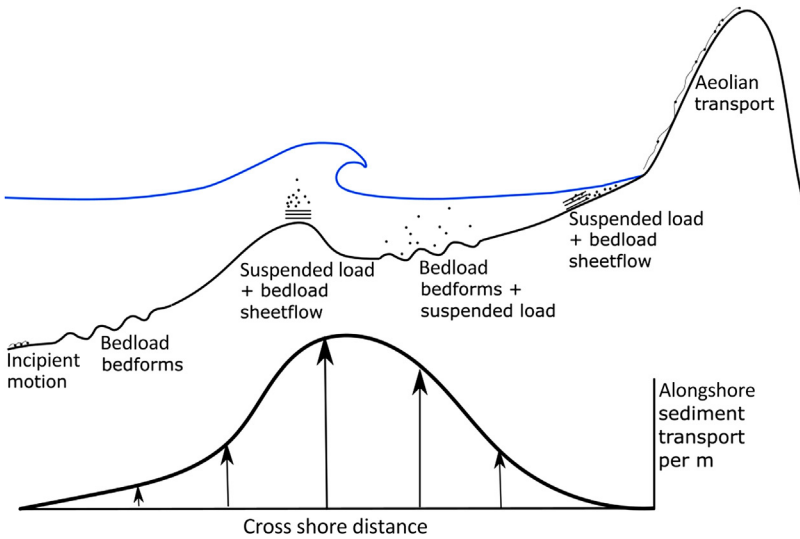

Figure 9.7 Cross-shore profile showing topographic gradients in cross-shore direction that involve bed level but also bedforms and sediment transport processes (top) and characteristic alongshore sediment transport magnitude relative to the cross-shore profile (bottom).

alongshore current is caused by a cross-shore gradient in the alongshore radiation stress in the surf zone (Longuet-Higgins, 1970). Additionally, alongshore currents can be driven by tide and alongshore varying wave heights that can cause an alongshore wave force and generate alongshore setup differences. Sediment concentrations in the surf zone are mostly driven by stirring due to the oscillating near-bed velocities in combination with the turbulence caused by breaking waves. Alongshore sediment transport is mainly induced by wave-related processes, and most studies and descriptions of alongshore sediment transport are therefore focused on the wave and surf zone properties.

Alongshore sediment transport can occur in both the positive and negative alongshore directions depending on the wave direction. The alongshore sediment transport in a sandy beach system varies in the cross-shore direction. Sediment concentrations are highest where most stirring due to turbulence takes place around the breakpoint, where waves start breaking. Also, wave breaking causes cross-shore gradients in radiation stresses to be large at this point and alongshore currents are relatively large. As a result, alongshore sediment transport is relatively large around the breakpoint.

Although the forcing mechanisms of alongshore sediment transport occur on the wave timescale, typical timescales on which the impacts of alongshore sediment transport are considered are weeks to decades. The gross sediment transport over a period of time is the sum of the transport in either of the two alongshore directional components. The net sediment transport is the sum of both directional components. The net sediment transport is often a small difference between two large numbers, which leads to large uncertainties when estimating the amount of net alongshore sediment transport at arbitrary locations.

9.4.1.1 *Estimating wave-driven alongshore sediment transport*

In practical situations, bulk formulations are often used for the estimation/quantification of alongshore sediment transport for engineering purposes. The most commonly used formula is the CERC formulation (CERC, 1984) that follows the principle that alongshore sediment transport (S_{lst}) is proportional to the alongshore wave power available for sediment transport (Komar, 1998). The CERC formula is equivalent in form to an energetics bedload approach to bulk alongshore transport (Inman and Bagnold, 1963). It should be noted that S_{lst} is commonly expressed in the deposited sediment volumes per time unit seconds (hence including pores [$m^3\ s^{-1}$]). The CERC formula reads:

$$S_{lst} = \frac{\rho K \sqrt{g/\gamma_b}}{16(\rho_s - \rho)(1-a)} H_{s,b}^{2.5} \sin 2\phi_b \tag{9.14}$$

where ρ is the density of the water, ρ_s is the density of sediment, g is the gravitation acceleration, γ_b is the breaker index, ϕ_b is the wave angle at breaking, $H_{s,b}$ is the significant wave height at breaking and K is an empirical coefficient. The volumetric mass of solid material is converted to deposited mass using the porosity index (a). K can be

calibrated using measurements where appropriate values that have been reported are in the range of 0.2 (Schoonees and Theron, 1997, 1993) to 0.39 (CERC, 1984). It has also been stated that the empirical coefficient might be dependent on surf similarity (Kamphuis and Readshaw, 1978). Mil-Homens et al. (2013) specified the dependency of K based on a polynomial relation with the surf similarity parameter. However, they state that much scatter continues to exist around the fitted relationship for the CERC formula (but also for other bulk formulae) that could be caused by profile shape, tidal range and local wind conditions, which are not taken into account in the bulk formulae. Despite caveats, the CERC formulation is nowadays still one of the most commonly used bulk sediment transport formulae.

More recently, Bayram et al. (2007) developed an energetics-suspended load approach to bulk alongshore transport. The result is a formulation in which alongshore currents are made explicit. In addition to the wave-driven currents, tide- and wind-driven currents can also be taken into account by using the product between local alongshore current velocity and the sediment concentration integrated through the vertical and across the surf zone:

$$S_{\mathrm{lst}} = 1/(1-a)\ \overline{u} \int_0^{x_b} \int_0^{h} c_s \, dz dx \tag{9.15}$$

where the x is in the cross-shore direction with 0 defined at the waterline, x_b is the location of the breakpoint and $\overline{u}$ is an estimate of a representative alongshore current velocity for transport.

Bayram et al. (2007) further used an energetics approach assuming that the work that is needed to keep the sediment in suspension is equal to a certain portion of the wave energy flux (EC) according to:

$$\varepsilon_w EC = (\rho_s - \rho)\, g w_s \int_0^{x_b} \int_0^{h} c_s \, dz dx \tag{9.16}$$

where ε_w representing the portion of wave energy used for the work, E is the wave energy per unit crest width and C is the wave group velocity. The right-hand side is the work needed to keep the sediment in suspension, which is given by the product of the concentration and the submerged weight of the sediment particles with the fall velocity.

By combining Eqs. (9.15) and (9.16) it is straightforward to calculate S_{lst}:

$$S_{\mathrm{lst}} = \frac{\varepsilon_w EC}{(\rho_s - \rho)(1-a)\, g w_s} \overline{u} \tag{9.17}$$

To account for the averaged alongshore current velocity due to oblique waves only, a simple alongshore momentum equation, linear wave theory and the assumption of a Dean profile can be used to determine a depth-average current according to Bayram et al. (2007):

$$\overline{u} = \frac{1}{x_b}\int_0^{x_b} u dx = \frac{5}{32}\frac{\pi\gamma_b\sqrt{g}}{c_f}A^{3/2}\sin\phi_b \tag{9.18}$$

where c_f is the friction coefficient and A is a parameter that describes the beach profile shape according to a Dean profile ($h = Ax^{2/3}$; Dean, 1991; van Rijn, 1993) and γ_b is the breaker index. Note that in Eq. (9.18), the lateral mixing of momentum is neglected and a single representative wave is assumed.

The combination between Eqs. (9.17) and (9.18), using an additional relationship between A and w_s by Kriebel et al. (1991), gives:

$$S_{lst} = \frac{135\ \gamma_b\pi\varepsilon}{256c_f}\frac{\rho\sqrt{g/\gamma_b}}{16(\rho_s-\rho)(1-a)}H_{s,b}^{2.5}\sin 2\phi_b \tag{9.19}$$

This expression is identical to the CERC formulation where:

$$K = \frac{135\ \gamma_b\pi\varepsilon}{256c_f} \tag{9.20}$$

linking the two approaches together when only considering wave-driven alongshore currents.

A range of time-varying wave heights and directions at breakpoint determine real-world sediment transport and applied numerical models (such as UNIBEST CL + , LITPACK and GENESIS) exist that provide elaborate estimations of cumulative alongshore sediment transport. Such models include time-varying conditions such as offshore wave height and direction, tide, wave period as well as profile shape and coastline orientation that influence the wave height and wave angle of incidence (both at breakpoint) and hence the sediment transport magnitude. Total transport during a period can be estimated by integrating over a discrete set of varying forcing conditions in time. Also, spatial gradients in time-aggregated alongshore sediment transport indicate erosive and accretive conditions.

The essence of describing alongshore sediment transport and the resulting relationships between angle of wave incidence and total sediment transport can be captured in an S–ϕ_b curve diagram (Fig. 9.8). The relationship between wave angle of incidence and sediment transport is often used at the core of the applied numerical models mentioned. Also, conceptual models based on the relationship have been used to explain naturally occurring coastline features such as high-angle wave-induced large-scale instabilities (Ashton et al., 2001).

9.4.2 Cross-shore sediment transport

Cross-shore sediment transport is relevant to many challenges related to sandy beach morphodynamics, including predicting beach and dune response to storms, the equilibrium beach profile, shoreline response to sea-level rise, seasonal shoreline changes

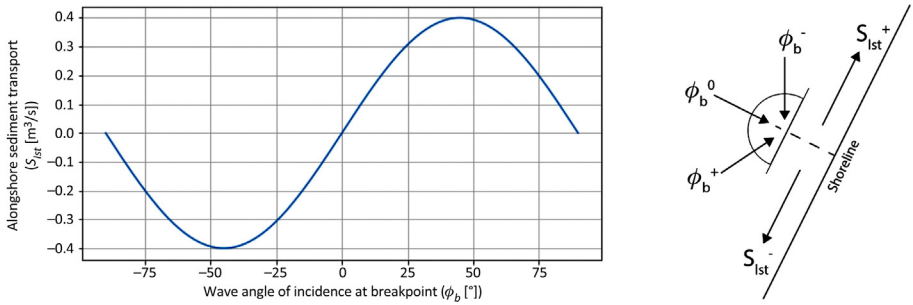

Figure 9.8 Left panel shows schematic representation of S–ϕ_b curve for an arbitrary wave height at breakpoint. Right panel shows schematic representation of different wave angles leading to different longshore sediment transport directions.

and possibly more (USACE, 2002). Both bedload and suspended load are important when considering cross-shore sediment transport, and each contributes at varying magnitudes and directions from the depth of closure to the shoreline (Fig. 9.7).

9.4.2.1 Mechanisms of cross-shore sediment transport

The detailed mechanisms of cross-shore sediment transport dynamics are very complex due to the strong variation of the constituent processes in time and space. In the surf zone, under normal/mild conditions a mix of processes occurs consisting of bed and suspended load transport due to undertow (bed return flow), bound and free long waves, short wave skewness and asymmetry in combination with breaking-induced turbulence (Bailard, 1981; Roelvink and Stive, 1989). During extreme conditions the undertow is dominant (Steetzel, 1993), although long wave effects (bound and free) cannot be ignored (van Thiel de Vries, 2009). Under higher and longer waves, as present during storms, a net offshore transport is generally observed. By contrast, milder waves give an onshore transport due to predominantly short wave skewness. Offshore of the surf zone (the middle and lower shoreface), a mix of bed and suspended load transport is also encountered, but here wave boundary layer streaming, bound long waves and short wave skewness can be expected to generate a dominant onshore transport.

Assuming for simplicity, that the cross-shore transport is proportional to a higher order odd velocity moment, as would follow from a quasi-steady transport formulation, the sediment load can be seen to be mainly stirred by short waves. The sediment is subsequently transported by the mean current or the long and short wave motion, leading to a net (wave-averaged) current-related or wave-related transport, respectively. The mean current could be the onshore-directed wave-induced near-bed streaming in non-breaking waves or the offshore-directed undertow in the surf zone. In such a quasi-steady approach, the contribution of the oscillatory part of the instantaneous velocity to the net transport, that is, the wave-related transport, is related to the short wave skewness as well as to the interaction between the long wave velocity and the short wave velocity variance (the latter will change periodically on the timescale of short wave groups).

Another important transport component in cross-shore direction (but not limited to the cross-shore direction) is driven by gravity. In the case of a sloping bed in cross-shore direction, the effects of slope on the initiation of motion have to be taken into account. Also, the transport directly induced by gravity when the grains have been set in motion can be significant. Therefore, in bedload formulations, sometimes a slope correction parameter is introduced (after Bagnold) which increases the transport rates for downslope transport and decreases the transport rates for upslope transport.

9.5 The present state and future challenges in sediment transport modelling

Comprehensive generic descriptions for quantifying the details of sediment transport do not exist due to the complexity caused by the discussed time-varying processes of suspended load and bedload sediment transport. To date, it is easier to predict offshore sediment transport (erosion) than onshore sediment transport in cases of beach building and recovery (Roelvink and Brøker, 1993). General methods that can be used to predict how sandy beaches evolve range from incorporating understanding of small-scale sediment transport processes in the case of process-based models to assuming a direct relation between beach shape and wave dissipation in equilibrium models.

Process-based models predict cross-shore sediment transport as a function of (detailed) hydrodynamic calculations. The processes of bedload and suspended load transport and the complex dependencies between grain size, local wave and current energy are incorporated. Examples of such models are XBeach (Roelvink et al., 2009), Delft3D (Lesser et al., 2004) and ROMS COAWST (Warner et al., 2008). Using the estimate of total sediment transport, process-based models estimate bed-level changes through gradients in sediment flux using Eq. (9.2). Such models need extensive tuning due to gaps in analytical understanding of cross-shore sediment transport processes and or feedback between processes.

Equilibrium models do not estimate sediment fluxes, but instead assume the beach profile to trend asymptotically towards an equilibrium shape based upon the wave energy dissipation and/or grain size. The widely used equilibrium profile assumption assumes that the beach profile trends to $Ax^{2/3}$, where x is the cross-shore distance and A is the beach shape factor, which is a function of wave energy dissipation and/or grain size (Bruun, 1954; Dean, 1991). More recently, the equilibrium model has been modelled by the first mode of the empirical orthogonal function about the beach profile mean (Ludka et al., 2015).

These methods are continuously under development and are becoming more and more robust to apply in practice with increased process knowledge and computing power in the future. Significant challenges continue to exist and specific directions to approach new concepts include two-phase flow models, coupled flow and particle models, and machine learning statistical models (such as described in Chapter 28). Such methods sometimes depend on different relationships for modelling sediment transport. Two-phase flow models numerically solve the Navier–Stokes equations for

a two-phase flow—fluid and sediment. For example, SedWaveFOAM models both water and sediment as fluids (Kim et al., 2018). Also, two-phase SPH models both water and sediment as discrete particles (Shi et al., 2017). In coupled flow-particle models the flow is numerically modelled with the Navier–Stokes equations and the particles act as discrete element springs with a higher density that are forced by the fluid (Calantoni et al., 2004). Bayesian statistic or other machine learning models, which are data-hungry statistical models, use existing data to learn the complex relationships and patterns of sediment transport (Plant and Holland, 2011).

9.6 Measuring the magnitude of sediment transport along sandy beaches

Direct measurements or measurement techniques of sediment transport that allow for systematic and precise observations of sediment transport that occur in field settings are not available. Instead, the models described so far can be used to estimate suspended sediment transport based on estimations of sediment concentrations (using calibrated optical backscatter devices or concentration samples) and flow velocities (using electromagnetic flow meters or acoustic Doppler current profilers or velocimeters). Bedload sediment transport via bedform migration can be measured using a set of sonar bathymetric scans or jet-ski surveys processed to estimate the bedload sediment flux (Traykovski et al., 1999; Hay and Mudge, 2005; de Schipper et al., 2016). Additionally, sheet flow, as observed on top of sandbars and in the swash zone, can be measured using conductivity cell profilers that detect changes in conductivity through the mobilised sediment bed between water and packed sand (Mieras et al., 2017).

The logistical and equipment costs that are involved with collecting field data limit the availability of data of sediment transport at sandy beaches. Even the most elaborate field campaigns have resulted in only a limited range of data points. Key field campaigns that are responsible for most of the data used in coastal studies are the series of Duck, North Carolina, US field campaigns, including Duck94, SandyDuck and SuperDuck (Birkemeier and Thornton, 1994), the Coast3D field campaign in the Netherlands (Soulsby, 1999), and other California, US-based experiments. There are several prominent long-term coastal evolution datasets, including the Pacific Northwest, USA (Oregon State University), Southern California, USA (Scripps Institute of Oceangraphy), Duck, NC, USA (US Army Corps Field Research Facility), the Southern Dutch coast, NL (TUDelft and Deltares) and Narrabeen, Australia (WRL-UNSW). Additionally, there have been several large-scale laboratory experiments with flume length of 100 m or greater, including in the Hinsdale Wave Lab at Oregon State University (CROSTEX), the DeltaFlume in the Netherlands (BARDEX I & II) and the Hydralab+ flume in Barcelona, Spain that have advanced understanding related to sediment transport.

A rare example of measured cross-shore sediment fluxes in the field during the Coast3D field campaign is shown in Fig. 9.9. A combination of measured flow velocities and sediment concentrations was used to estimate wave-averaged sediment

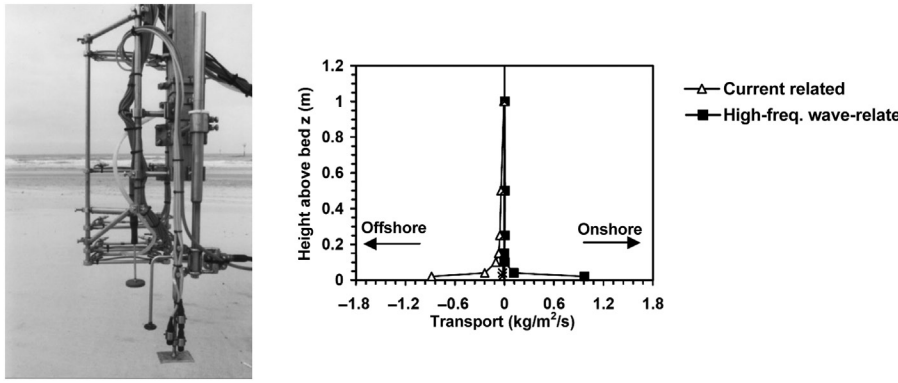

Figure 9.9 Left photo shows an example of an array with optical backscatter devices and electromagnetic current meters used to gather data on current speed and sediment concentration. Right figure shows an example of transport measurements in cross-shore direction after (Grasmeijer, 2002).
Source: Both images courtesy of Bart Grasmeijer.

fluxes at a sandy beach. The signal reveals that both the magnitude and direction of 'current-related' transport and 'wave-related' transport (showing onshore transport due to nonlinear waves) vary over the vertical, as described in Section 9.4.2. Measured current-related sediment transport was in the offshore direction depitcing undertow. Measured wave-related transport was in onshore direction due to nonlinear waves. In both cases, sediment transport is relatively large close to the sediment bed highlighting the importance of resolving near-bed processes when measuring and modelling sediment transport.

9.7 Conclusions and outlook

The concepts that are presented in this chapter give an introduction, and a perspective, of the sediment transport processes used to describe mechanisms for evolution of sandy beaches. Sediment transport in the cross-shore and the alongshore directions over varying length and timescales can be estimated using a combination of suspended load and bedload formulations. Given the complicated range of the relevant spatiotemporal scales for sediment transport processes at sandy beaches, a unifying theory that involves all concepts available would be an immense challenge to achieve in the near future. Ongoing scientific progress steadily builds towards additional understanding, comprehensive concepts, and analysis and modelling techniques.

From a scientific perspective, there is currently much work still to be done regarding the quantification of sediment transport due to hydrodynamic forcing (van Rijn et al., 2013). New possibilities of executing detailed measurements are emerging and more detailed process concepts are being formulated based on new insights. Amongst those recent insights are the role of grain size distributions in specific cases

(Huisman et al., 2016), the role of natural and human-induced variations in large-scale coastal morphology (Luijendijk et al., 2017), the role of bedforms (Wengrove et al., 2019, 2018), the role of wave shape in sheet flow processes (Mieras et al., 2017), the role of complex hydrodynamic forcing conditions (Meirelles et al., 2018) and the interaction between marine and aeolian sediment transport (Cohn et al., 2019). In addition to that, computational infrastructure (through, for example, parallel processing techniques) now allows increasingly detailed numerical simulations of individual sediment transport processes (see, for instance, Luijendijk et al., 2019). These new developments continue to provide valuable contributions towards the field of coastal sediment transport, building an ever-evolving and expanding knowledge base.

References

Ashton, A., Murray, A.B., Arnoult, O., 2001. Formation of coastline features by large-scale instabilities induced by high-angle waves. Nature 414, 296–300. doi: 10.1038/35104541.

Bagnold, R.A., 1966. An approach to the sediment transport problem from general physics. Geological Survey Professional Paper 422-II. Washington, DC.

Bailard, J.A., 1981. An energetics total load sediment transport model for a plane sloping beach. J. Geophys. Res. Atmos. 86, 938–954.

Bailard, J.A., Inman, D.L., 1981. An energetics bedload model for a plane sloping beach: local transport. J. Geophys. Res. Ocean 86, 2035–2043. doi: 10.1029/JC086iC03p02035.

Bayram, A., Larson, M., Hanson, H., 2007. A new formula for the total longshore sediment transport rate. Coast. Eng. 54, 700–710. doi: 10.1016/j.coastaleng.2007.04.001.

Birkemeier, W.A., Thornton, E.B., 1994. The DUCK94 nearshore field experiment. Coast. Dyn. 94, 815–821.

Bowen, A.J., 1980. Simple models of nearshore sedimentation: beach profiles and long-shore bars. In: McCann, S.B. (Ed.), The Coastline Canada. Geological Survey of Canada, pp. 1–11.

Bruun, P., 1954. Coast Erosion and the Development of Beach Profiles. US Beach Erosion Board, Washington, DC.

Calantoni, J., Todd Holland, K., Drake, T.G., 2004. Modelling sheet–flow sediment transport in wave–bottom boundary layers using discrete–element modelling. Philos. Trans. R. Soc. London Ser. A Math. Phys. Eng. Sci. 362, 1987–2001. doi: 10.1098/rsta.2004.1427.

Camenen, B., Larson, M., 2007. A unified sediment transport formulation for coastal inlet application. ERDC-CHL-C. U.S. US Army Engineer Research and Development Center, Vicksburg.

CERC, 1984. Shore protection manual. Army Engineer Waterways Experiment Station, Vicksburg, MS. 2v.

Cohn, N., Hoonhout, B., Goldstein, E., De Vries, S., Moore, L., Durán Vinent, O., Ruggiero, P., 2019. Exploring marine and aeolian controls on coastal foredune growth using a coupled numerical model. J. Mar. Sci. Eng. 7, 13. doi: 10.3390/jmse7010013.

de Schipper, M.A., de Vries, S., Ruessink, G., de Zeeuw, R.C., Rutten, J., van Gelder-Maas, C., Stive, M.J.F., 2016. Initial spreading of a mega feeder nourishment: observations of the Sand Engine pilot project. Coast. Eng. 111, 23–38. doi: 10.1016/j.coastaleng.2015.10.011.

Dean, R.G., 1991. Equilibrium beach profiles: characteristics and applications. J. Coast. Res. 7doi: 10.2307/4297805, 53–48.

Foster, D.L., Bowen, A.J., Holman, R.A., Natoo, P., 2006. Field evidence of pressure gradient induced incipient motion. J. Geophys. Res. 111, C05004. doi: 10.1029/2004JC002863.

Frank, D., Foster, D., Sou, I.M., Calantoni, J., Chou, P., 2015. Lagrangian measurements of incipient motion in oscillatory flows. J. Geophys. Res. Ocean 120, 244–256. doi: 10.1002/2014JC010183.

Grasmeijer, B., 2002. Process-based cross-shore modelling of barred beaches. Netherlands Geogr. Stud. 302, 251.

Hay, A.E., Mudge, T., 2005. Principal bed states during SandyDuck97: occurrence, spectral anisotropy, and the bed state storm cycle. J. Geophys. Res. Ocean 110, C03013.doi: 10.1029/2004JC002451.

Hoefel, F., Elgar, S., 2003. Wave-induced sediment transport and sandbar migration. Science 299, 1885–1887. doi: 10.1126/science.1081448.

Hsu, T.-J., Elgar, S., Guza, R.T., 2006. Wave-induced sediment transport and onshore sandbar migration. Coast. Eng. 53, 817–824. doi: 10.1016/j.coastaleng.2006.04.003.

Huisman, B.J.A., de Schipper, M.A., Ruessink, B.G., 2016. Sediment sorting at the Sand Motor at storm and annual time scales. Mar. Geol. 381, 209–226. doi: 10.1016/j.margeo.2016.09.005.

Inman, D.L., Bagnold, R.A., 1963. Beach and Nearshore Processes; Part II: Littoral Processes. Hill, M.N. (Ed.), The Sea, pp. 529–553.

Kamphuis, J.W., Readshaw, J.S., 1978. A model study of alongshore sediment transport rate. Coast. Eng. Proc. 1, 99. doi: 10.9753/icce.v16.99.

Kim, Y., Cheng, Z., Hsu, T.-J., Chauchat, J., 2018. A numerical study of sheet flow under monochromatic nonbreaking waves using a free surface resolving Eulerian two-phase flow model. J. Geophys. Res. Ocean 123, 4693–4719. doi: 10.1029/2018JC013930.

Komar, P.D., 1998. Beach processes and sedimentation, second ed., Prentice-Hall, Englewood-Cliffs, doi: 10.5860/CHOICE.36-1592.

Kriebel, D.L., Kraus, N.C., Larson, M., 1991. Engineering methods for predicting beach profile response. Proceedings of Coastal Sediments '91. American Society of Civil Engineers, pp. 557–571.

Lesser, G.R., Roelvink, J.A., van Kester, J.A.T.M., Stelling, G.S., 2004. Development and validation of a three-dimensional morphological model. Coast. Eng. 51, 883–915.

Longuet-Higgins, M.S., 1970. Longshore currents generated by obliquely incident sea waves: 1. J. Geophys. Res. 75, 6778–6789. doi: 10.1029/JC075i033p06778.

Ludka, B.C., Guza, R.T., O'Reilly, W.C., Yates, M.L., 2015. Field evidence of beach profile evolution toward equilibrium. J. Geophys. Res. Ocean 120, 7574–7597. doi: 10.1002/2015JC010893.

Luijendijk, A., Schipper, M., Ranasinghe, R., 2019. Morphodynamic acceleration techniques for multi-timescale predictions of complex sandy interventions. J. Mar. Sci. Eng. 7, 78. doi: 10.3390/jmse7030078.

Luijendijk, A.P., Ranasinghe, R., de Schipper, M.A., Huisman, B.A., Swinkels, C.M., Walstra, D.J.R., Stive, M.J.F., 2017. The initial morphological response of the Sand Engine: a process-based modelling study. Coast. Eng. 119, 1–14. doi: 10.1016/j.coastaleng.2016.09.005.

Meirelles, S., Henriquez, M., Reniers, A., Luijendijk, A.P., Pietrzak, J., Horner-Devine, A.R., Souza, A.J., Stive, M.J.F., 2018. Cross-shore stratified tidal flow seaward of a mega-nourishment. Estuar. Coast. Shelf Sci. 200, 59–70. doi: 10.1016/j.ecss.2017.10.013.

Meyer-Peter, E., Muller, R., 1948. Formulas for bed-load transport. AHSR 2nd Meeting, Appendix 2. IAHR, Stockholm.

Mieras, R.S., Puleo, J.A., Anderson, D., Cox, D.T., Hsu, T.-J., 2017. Large-scale experimental observations of sheet flow on a sandbar under skewed-asymmetric waves. J. Geophys. Res. Ocean 122, 5022–5045. doi: 10.1002/2016JC012438.

Mil-Homens, J., Ranasinghe, R., van Thiel de Vries, J.S.M., Stive, M.J.F., 2013. Re-evaluation and improvement of three commonly used bulk longshore sediment transport formulas. Coast. Eng. 75, 29–39. doi: 10.1016/j.coastaleng.2013.01.004.

Nielsen, P., 1992. Coastal Bottom Boundary Layers and Sediment Transport. World Scientific, River Edge, NJ.

Parker, G., Paola, C., Leclair, S., 2000. Probabilistic exner sediment continuity equation for mixtures with no active layer. J. Hydraul. Eng. 126, 818–826. doi: 10.1061/(ASCE)0733-9429(2000)126:11(818).

Plant, N.G., Holland, K.T., 2011. Prediction and assimilation of surf-zone processes using a Bayesian network: Part II: inverse models. Coast. Eng. 58, 256–266. doi: 10.1016/j.coastaleng.2010.11.002.

Ribberink, J.S., 1998. Bed-load transport for steady flows and unsteady oscillatory flows. Coast. Eng. 34, 59–82. doi: 10.1016/S0378-3839(98)00013-1.

Rodríguez-Abudo, S., Foster, D.L., 2014. Unsteady stress partitioning and momentum transfer in the wave bottom boundary layer over movable rippled beds. J. Geophys. Res. Ocean 119, 8530–8551. doi: 10.1002/2014JC010240.

Roelvink, D., Reniers, A., van Dongeren, A., van Thiel de Vries, J., McCall, R., Lescinski, J., 2009. Modelling storm impacts on beaches, dunes and barrier islands. Coast. Eng. 56, 1133–1152. doi: 10.1016/j.coastaleng.2009.08.006.

Roelvink, J.A., Brøker, I., 1993. Cross-shore profile models. Coast. Eng. 21, 163–191. doi: 10.1016/0378-3839(93)90049-E.

Roelvink, J.A., Stive, M.J.F., 1989. Bar-generating cross-shore flow mechanisms on a beach. J. Geophys. Res. 94, 4785–4800. doi: 10.1029/JC094iC04p04785.

Schoonees, J.S., Theron, A.K., 1997. Improvement of the most accurate longshore transport formula. In: Coastal Engineering 1996. American Society of Civil Engineers, New York, NY, pp. 3652–3665, doi: 10.1061/9780784402429.282.

Schoonees, J.S., Theron, A.K., 1993. Review of the field-data base for longshore sediment transport. Coast. Eng. 19, 1–25. doi: 10.1016/0378-3839(93)90017-3.

Shi, H., Yu, X., Dalrymple, R.A., 2017. Development of a two-phase SPH model for sediment laden flows. Comput. Phys. Commun. 221, 259–272. doi: 10.1016/j.cpc.2017.08.024.

Shields, A., 1936. Anwendung der Aehnlichkeitsmechanik und der Turbulenzforschung auf die Geschiebebewegung. PhD Thesis Tech. University of Berlin.

Sleath, J.F., 1999. Conditions for plug formation in oscillatory flow. Cont. Shelf Res. 19, 1643–1664. doi: 10.1016/S0278-4343(98)00096-X.

Soulsby, R.L., 1999. Coastal sediment transport: the COAST3D Project. In: Coastal Engineering 1998. American Society of Civil Engineers, Reston, VA, pp. 2548–2558, doi: 10.1061/9780784404119.192.

Steetzel, H.J., 1993. Cross shore transport during storm surges. PhD dissertation, Delft University of Technology.

Svendsen, I.A., Lorenz, R.S., 1989. Velocities in combined undertow and longshore currents. Coast. Eng. 13, 55–79. doi: 10.1016/0378-3839(89)90032-X.

Traykovski, P., Hay, A.E., Irish, J.D., Lynch, J.F., 1999. Geometry, migration, and evolution of wave orbital ripples at LEO-15. J. Geophys. Res. Ocean 104, 1505–1524. doi: 10.1029/1998JC900026.

USACE, 2002. Coastal engineering manual, EM 1110-2-1100, Part III, doi: 10.1093/intimm/dxs026.

van der A, D.A, Ribberink, J.S., van der Werf FJ.J., O'Donoghue, T., Buijsrogge, R.H., Kranenburg, W.M., 2013. Practical sand transport formula for non-breaking waves and currents. Coast. Eng. 76, 26–42. doi: 10.1016/j.coastaleng.2013.01.007.

van Rijn, L.C., 2007. United view of sediment transport by currents and waves I: initiation of motion, bed roughness and Bed load transport. J. Hydraul. Eng. 133, 649–667.

van Rijn, L.C., 1993. Principles of Sediment Transport in Rivers, Estuaries and Coastal Seas. Aqua Publications, Amsterdam.

van Rijn, L.C., Ribberink, J.S., Van der Werf, J., Walstra, D.J.R., 2013. Coastal sediment dynamics: recent advances and future research needs. J. Hydraul. Res. 51, 475–493. doi: 10.1080/00221686.2013.849297.

van Thiel de Vries, J.S.M., 2009. Dune erosion during storm surges. PhD Dissertation, Delft University of Technology.

Warner, J.C., Sherwood, C.R., Signell, R.P., Harris, C.K., Arango, H.G., 2008. Development of a three-dimensional, regional, coupled wave, current, and sediment-transport model. Comput. Geosci. 34, 1284–1306. doi: 10.1016/j.cageo.2008.02.012.

Wengrove, M.E., Foster, D.L., Lippmann, T.C., de Schipper, M.A., Calantoni, J., 2019. Observations of bedform migration and bedload sediment transport in combined wave-current flows. J. Geophys. Res. Ocean 124.doi: 10.1029/2018JC014555, 2018JC014555.

Wengrove, M.E., Foster, D.L., Lippmann, T.C., de Schipper, M.A., Calantoni, J., 2018. Observations of time-dependent bedform transformation in combined wave-current flows. J. Geophys. Res. Ocean 123, 7581–7598. doi: 10.1029/2018JC014357.

Yeh, H., Mason, H.B., 2014. Sediment response to tsunami loading: mechanisms and estimates. Géotechnique 64, 131–143. doi: 10.1680/geot.13.P.033.